

Radiation Pressure Driven Galactic Winds from Self-Gravitating Discs

Dong Zhang^{1*} and Todd A. Thompson^{1,2†}

¹*Department of Astronomy, The Ohio State University, 140 West 18th Avenue, Columbus, OH 43210, USA*

²*Center for Cosmology & Astro-Particle Physics, The Ohio State University, Columbus, Ohio 43210, USA*

30 March 2022

ABSTRACT

We study large-scale winds driven from uniformly bright self-gravitating discs radiating near the Eddington limit. We show that the ratio of the radiation pressure force to the gravitational force increases with height above the disc surface to a maximum of twice the value of the ratio at the disc surface. Thus, uniformly bright self-gravitating discs radiating at the Eddington limit are fundamentally unstable to driving large-scale winds. These results contrast with the spherically symmetric case, where super-Eddington luminosities are required for wind formation. We apply this theory to galactic winds from rapidly star-forming galaxies that approach the Eddington limit for dust. For hydrodynamically coupled gas and dust, we find that the asymptotic velocity of the wind is $v_\infty \simeq 1.5 v_{\text{rot}}$ and that $v_\infty \propto \text{SFR}^{0.36}$, where v_{rot} is the disc rotation velocity and SFR is the star formation rate, both of which are in agreement with observations. However, these results of the model neglect the gravitational potential of the surrounding dark matter halo and a (potentially massive) old passive stellar bulge or extended disc, which act to decrease v_∞ . A more realistic treatment shows that the flow can either be unbound, or bound, forming a “fountain flow” with a typical turning timescale of $t_{\text{turn}} \sim 0.1 - 1$ Gyr, depending on the ratio of the mass and radius of the rapidly star-forming galactic disc relative to the total mass and break (or scale) radius of the dark matter halo or bulge. We provide quantitative criteria and scaling relations for assessing whether or not a rapidly star-forming galaxy of given properties can drive unbound flows via the mechanism described in this paper. Importantly, we note that because t_{turn} is longer than the star formation timescale (gas mass/star formation rate) in the rapidly star-forming galaxies and ultra-luminous infrared galaxies for which our theory is most applicable, if rapidly star-forming galaxies are selected as such, they may be observed to have strong outflows along the line of sight with a maximum velocity v_{max} comparable to $\sim 1.5 v_{\text{rot}}$, even though their winds are eventually bound on large scales.

Key words: galaxies: starburst — galaxies: formation — galaxies: intergalactic medium — galaxies: haloes

1 INTRODUCTION

Galactic-scale winds are ubiquitous in rapidly star-forming galaxies in both the local and high-redshift universe (Heckman et al. 1990; Heckman et al. 2000; Pettini et al. 2001, 2002; Shapley et al. 2003; Rupke et al. 2005; Sawicki et al. 2008). They are important for determining the chemical evolution of galaxies and the mass-metallicity relation (Dekel & Silk 1986; Tremonti et al. 2004; Erb et al.

2006; Finlator & Davé 2008; Peeples & Shankar 2011), and as a primary source of metals in the intergalactic medium (IGM; e.g., Aguirre et al. 2001). Moreover, galactic winds are perhaps the most extreme manifestation of the feedback between star formation in a galaxy and its interstellar medium (ISM). This feedback mechanism is crucial for understanding galaxy formation and evolution over cosmic time (Springel & Hernquist 2003; Oppenheimer & Davé 2006; Oppenheimer & Davé 2008; Oppenheimer et al. 2010).

The most well-developed model for galactic winds from rapidly star-forming galaxies is the supernova-driven model

* E-mail: dzhang@astronomy.ohio-state.edu

† Alfred P. Sloan Fellow

of Chevalier & Clegg (1985), which assumes that the energy from multiple stellar winds and core-collapse supernovae in the starburst is efficiently thermalized. The resulting hot flow drives gas out of the host, sweeping up the cool ISM (Heckman, Lehnert & Armus 1993; De Young & Heckman 1994; Strickland & Stevens 2000; Strickland et al. 2002; Strickland & Heckman 2009; Fujita et al. 2009). Although this model is successful in explaining the X-ray properties of rapidly star-forming galaxies, the recent observational results that galaxies with higher star formation rates (SFRs) accelerate the absorbing cold gas clouds to higher velocities ($v \propto \text{SFR}^{0.35}$) and that the wind velocity is correlated with the galaxy escape velocity may challenge the traditional hypothesis that the cool gas is accelerated by the ram pressure of the hot supernova-heated wind, whose X-ray emission temperature varies little with SFR, circular velocity, and host galaxy mass, indicating a critical galaxy mass below which most of the hot wind escapes (e.g., Martin 1999). These new observations may instead favor momentum-driven or radiation pressure-driven models for the wind physics (e.g., Martin 2005; Weiner et al. 2009; Murray, Quataert & Thompson 2005 [hereafter MQT05]).

The model that galactic winds may be driven by momentum deposition provided by radiation pressure from the continuum absorption and scattering of starlight on dust grains was developed by MQT05. However, the conclusions of MQT05 are based on an assumed isothermal potential and spherical geometry, and are thus most appropriate for bright elliptical/spheroidal galaxies in formation. On the other hand, the theory of radiation-driven winds from accretion discs from the stellar to galactic scales has also been studied (e.g., Tajima & Fukue 1996, 1998; Proga, Stone & Drew 1998, 1999; Proga 2000, 2003), but none of these works considered radiation from self-gravitating discs.

In this paper we answer the question of whether or not large-scale winds can be driven by radiation pressure from self-gravitating discs radiating near the Eddington limit. These considerations are motivated by the work of Thompson, Quataert & Murray (2005; TQM05), who argued that radiation pressure on dust is the dominant feedback mechanism in rapidly star-forming galaxies, and that in these systems star formation is Eddington-limited. For simplicity, throughout this paper we assume that the disc is of uniform brightness and surface density. In Section 2, we show that such discs are fundamentally unstable to wind formation because the radiation pressure force dominates gravity in the vertical direction above the disc surface. This result is qualitatively different from the well-known case in spherical symmetry. In Section 2, we also discuss the applicability of this model to rapidly star-forming galaxies and then calculate the terminal velocity of the wind along the disc pole, and its dependence on both the SFR and galaxy escape velocity. In Section 3, we assess the importance of a spherical stellar bulge or extended passive disc, and dark matter halo potential. In Section 4, we discuss the 3-dimensional wind structure and estimate the total wind mass loss rate. We discuss our findings and conclude in Section 5.

2 RADIATION-DRIVEN WINDS & THE TERMINAL VELOCITY

We consider the idealized model problem of a disc with uniform brightness and total surface density: $I(r \leq r_{\text{rad}}) = I$ and $\Sigma(r \leq r_D) = \Sigma$, where r_{rad} and r_D define the outer radius of the luminous and gravitating portion of the disc, respectively. The flux-mean opacity to absorption and scattering of photons is κ . The gravitational force along the polar axis above the disc is

$$\begin{aligned} f_{\text{grav}}(z) &= -2\pi G \Sigma \int_0^{r_D} \frac{z r dr}{(r^2 + z^2)^{3/2}} \\ &= -2\pi G \Sigma \left(1 - \frac{z}{\sqrt{z^2 + r_D^2}} \right), \end{aligned} \quad (1)$$

and the vertical radiation force along the pole is

$$f_{\text{rad}}(z) = \frac{2\pi \kappa I}{c} \int_0^{r_{\text{rad}}} \frac{z^2 r dr}{(r^2 + z^2)^2} = \frac{\pi \kappa I}{c} \frac{r_{\text{rad}}^2}{z^2 + r_{\text{rad}}^2}. \quad (2)$$

The extra factor of $z/\sqrt{r^2 + z^2}$ in the radiation force integral compared with the gravitational force is the projection cosine factor $\cos \theta$ such that $df_{\text{rad}} \propto \cos \theta d\Omega$, where θ is the angle between the z -axis direction and the direction of the solid angle $d\Omega$ at the disk surface (Rybicki & Lightman 1979; see also Proga, Stone & Drew 1998; Tajima & Fukue 1998). Thus, the Eddington ratio along the pole $\Gamma(z) = |f_{\text{rad}}(z)/f_{\text{grav}}(z)|$ as a function of height z is given by

$$\Gamma(z) = \Gamma_0 \left(\frac{r_{\text{rad}}}{r_D} \right)^2 \left(\frac{z^2 + r_D^2}{z^2 + r_{\text{rad}}^2} + \frac{z\sqrt{z^2 + r_D^2}}{z^2 + r_{\text{rad}}^2} \right), \quad (3)$$

where $\Gamma_0 = \Gamma(z=0) = \kappa I/(2cG\Sigma)$ is the Eddington ratio at the disc center. A disc at the Eddington limit ($\Gamma_0 = 1$) requires $I_{\text{Edd}} = 2cG\Sigma/\kappa$, or flux $F_{\text{Edd}} = 2\pi cG\Sigma/\kappa$. If $r_{\text{rad}}/r_D > 1/\sqrt{2} \simeq 0.7$, then $\Gamma(z)$ increases along the z -axis above the disc. In particular, for $r_{\text{rad}} \simeq r_D$, the radiation force becomes twice the gravitational force as $z \rightarrow \infty$:

$$\Gamma_{\infty} = \Gamma(z \rightarrow \infty) = 2. \quad (4)$$

Because $\Gamma(z)$ increases monotonically with z , an infinitesimal displacement of a test particle in the vertical direction yields a net vertical acceleration, and the disc is thus unstable to wind formation. This result for discs is qualitatively different from the spherical case with a central point source where $\Gamma = f_{\text{rad}}/f_{\text{grav}}$ is constant with radius.

In the more realistic case we consider an exponential disc with surface brightness $I = I_0 \exp(-r/R_{\text{rad}})$ and surface density $\Sigma = \Sigma_0 \exp(-r/R_D)$. The disc has approximately uniform brightness for $r < R_D$ and uniform density for $r < R_{\text{rad}}$, while the brightness and mass distribution cut off for $r \simeq R_{\text{rad}}$ and $r \simeq R_D$ respectively. The vertical radiation and gravitational forces along the pole above the exponential disc can be calculated by multiplying the integrals in equations (1) and (2) by the exponential terms $\exp(-r/R_D)$ and $\exp(-r/R_{\text{rad}})$ respectively. As a result, in this case the Eddington ratio becomes a function of R_{rad}/R_D . We obtain the Eddington ratio along the pole $\Gamma(z \rightarrow \infty) = 2\Gamma(z=0)$ if $R_{\text{rad}} = R_D$, and $\Gamma(z \rightarrow \infty) \leq \Gamma(z=0)$ if $R_D \geq \sqrt{2}R_{\text{rad}}$. Therefore the exponential disc gives a result similar to the uniform disc case in that $\Gamma(z)$ increases monotonically only if $R_D < \sqrt{2}R_{\text{rad}} \simeq 1.4R_{\text{rad}}$, otherwise the disc is not promising to drive a wind because the gravitational force domi-

nates over the outward radiation pressure force. Then we take $r_D = \sqrt{2}R_{\text{rad}}$ and refer to the region outside of the active and bright region ($r \gtrsim \sqrt{2}R_{\text{rad}}$) as the “extended passive disc”, and we discuss it together with the effects of an old stellar bulge and dark matter halo in Section 3.

Hereafter we adopt the uniform disc model. If we consider the motion of a test particle in the outflow, the velocity along the z -axis can be written as

$$\frac{v(z)^2 - v_0^2}{4\pi G \Sigma r_D} = \hat{r} \Gamma_0 \arctan\left(\frac{\hat{z}}{\hat{r}}\right) - \left(1 + \hat{z} - \sqrt{1 + \hat{z}^2}\right), \quad (5)$$

where $\hat{r} = r_{\text{rad}}/r_D$, $\hat{z} = z/r_D$, and v_0 is initial vertical velocity. The first term on the right side of equation (5) is the “radiation potential” along the pole, while the second term is the gravitational potential. The right side is always positive if $\Gamma_0 \geq 1$ and $\hat{r}\Gamma_0 > 2/\pi \approx 0.64$, and thus the gas can be accelerated to infinity. On the other hand, an unbound outflow is still possible in the sub-Eddington case $\Gamma_0 < 1$ if the initial velocity v_0 is sufficiently large to escape the gravitational potential above the disc until reaching the critical height z^* where $\Gamma(z^*) = 1$, because the gas is decelerated from its initial v_0 until it reaches z^* , it will be accelerated to infinity if $v(z^*) \geq 0$. Using this constraint, we calculate the minimum v_0 required to drive an unbound wind in the sub-Eddington case, and the critical height z^* where the wind profile acceleration changes sign. Figure 1 shows the results. We introduce a characteristic velocity $v_c = \sqrt{4\pi G \Sigma r_D}$. The calculation is applied for $v_\infty = v(z \rightarrow \infty) \geq v_0$, or $\hat{r}\Gamma_0 > 2/\pi \simeq 0.64$. In this case the wind can be accelerated at infinity. The important point here is that for a disc with sub-Eddington brightness, and non-zero vertical velocity v_0 , the gas can be first decelerated and then accelerated to infinity. For the typical random initial velocities of gas in galaxies $\rho v_0^2 \sim \pi G \Sigma^2$, we have $v_0/v_c \sim (h/2r_D)^{1/2} \sim 0.22(r/r_D)^{1/2}$, where the galactic thickness scale $h = 0.1r$ has been assumed for the second equality (Downes & Solomon 1998). For this reason we expect that even somewhat sub-Eddington discs can drive outflows, as shown in Figure 1. In contrast with the spherical case for which $v_z^2 - v_0^2 \propto \Gamma_0 - 1$, uniformly bright self-gravitating discs allow the gas above the disc to be accelerated for the case with $\Gamma_0 = 1$ or even for some sub-Eddington cases. In Section 4, we show the 3-dimensional trajectories of wind particles launched from both Eddington and sub-Eddington discs.

We wish to apply this simple theory to rapidly star-forming galaxies, which may reach the Eddington limit for dust (TQM05). However, this application depends on the extent to which a disc-like collection of point sources of radiation (stars) may be treated as a uniformly bright disc. In the limit that the dusty gas of rapidly star-forming galaxies is optically-thick to the re-radiated FIR emission in galactic discs ($\Sigma \gtrsim 0.1 - 1 \text{ g cm}^{-2}$; $\kappa_{\text{FIR}} \sim 1 - 10 \text{ cm}^2 \text{ g}^{-1}$; see TQM05), as is reached in ULIRGs, the self-gravitating discs around bright AGN, and some rapidly star-forming galaxies, the approximation of a uniform brightness disc is likely valid. However, for $\Sigma \lesssim 10^{-3} \text{ g cm}^{-2}$ ($\kappa_{\text{UV}} \sim 10^3 \text{ cm}^2 \text{ g}^{-1}$), the disc is optically thin to the UV radiation of massive stars. Because the massive stars are point sources and dominate the galaxy’s bolometric luminosity, the approximation of a 2-dimensional uniformly bright disc breaks down. In

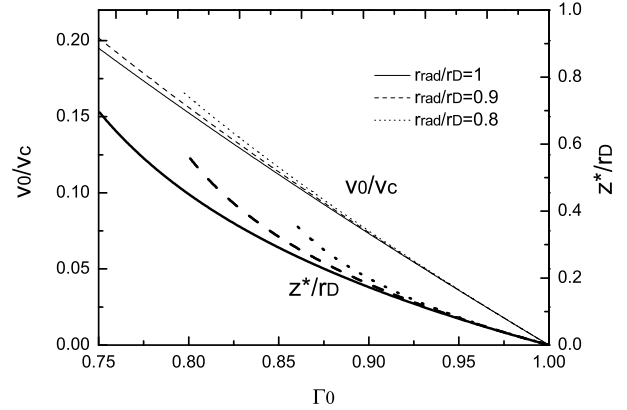


Figure 1. Minimum initial velocity v_0/v_c to drive unbound winds (thin lines), and the critical height z^* turning the gas from deceleration to accelerations (thick lines) as a function of Eddington ratio Γ_0 in the sub-Eddington case $2/(\pi\hat{r}) < \Gamma_0 < 1$, where $\hat{r} = r_{\text{rad}}/r_D = 1, 0.9$ and 0.8 .

the intermediate regime $10^{-3} \lesssim \Sigma \lesssim 0.1 - 1 \text{ g cm}^{-2}$,¹ the disc is optically-thick to UV radiation, but optically-thin to the re-radiated FIR, the application of the simple uniformly bright disc model is tentative, as the fraction of the light that is absorbed and scattered in the gas depends on the distribution of the sources relative to the dusty gas, the inter-star spacing relative to the vertical scale of the dusty gas, and the grain size distribution, which affects the overall scattering albedo. We save a detailed investigation of the intermediate case for a future work, but here note two important points: (1) even for low- Σ galaxies, the fraction of diffuse (potentially scattered) UV light may be substantial (Thilker et al. 2005), and (2) if a finite thickness disc is uniformly emissive and absorptive, then $\kappa_{\text{UV}} F_{\text{UV}} \sim \kappa_{\text{UV}} F_{\text{tot}}/\tau_{\text{UV}} \sim F_{\text{tot}}/\Sigma > \kappa_{\text{FIR}} F_{\text{FIR}}$, where $\tau_{\text{UV}} \sim \kappa_{\text{UV}} \Sigma$ and F_{tot} , F_{UV} , and F_{FIR} are the total, UV, and FIR fluxes, respectively. The radiation pressure force above the disc is thus dominated by UV emission from the “skin” of the disc (the $\tau_{\text{UV}} \sim 1$ surface). Therefore, if the total flux is equal to the Eddington flux – $F_{\text{tot}} = 2\pi G c \Sigma / \kappa$, where κ is the flux-mean opacity – then the escaping UV radiation is also at Eddington: $F_{\text{UV}} \sim F_{\text{tot}}/\tau_{\text{UV}} \sim 2\pi G c \Sigma / (\tau_{\text{UV}} \kappa) \sim 2\pi G c \Sigma / \kappa_{\text{UV}}$. For these reasons, the model of a uniformly bright disc may apply even when $\Sigma < 0.1 - 1 \text{ g cm}^{-2}$ and the medium is not optically thick to the reradiated FIR.

To proceed with our application to rapidly star-forming galaxies, the characteristic velocity v_c is written as

$$v_c = \sqrt{4\pi G \Sigma r_D} = 500 \text{ km s}^{-1} \Sigma_0^{1/2} r_{D,1\text{kpc}}^{1/2}, \quad (6)$$

where we take $\Sigma_0 = \Sigma/1 \text{ g cm}^{-2} = \Sigma/(4800 \text{ M}_\odot \text{ pc}^{-2})$, and $r_{D,1\text{kpc}} = r_D/1 \text{ kpc}$. Momentarily neglecting the importance of the surrounding dark matter halo, or a potentially massive old stellar bulge or extended passive disc (which we evaluate in Section 3), from equation (5) with $\Gamma_0 = 1$ and $r_{\text{rad}} \simeq r_D$, the asymptotic terminal velocity along the pole is

¹ These bounds on Σ depend linearly on the gas-to-dust ratio.

$$v_\infty = v_c \sqrt{\pi/2 - 1} \simeq 380 \text{ km s}^{-1} \Sigma_0^{1/2} r_{D,1\text{kpc}}^{1/2}. \quad (7)$$

This expression for v_∞ can be related to the star formation rate (SFR) using the Schmidt law, which relates the star formation surface density and gas surface density in galactic discs: $\Sigma_{\text{SFR}} \propto \Sigma_{\text{gas}}^{1.4}$ (Kennicutt 1998). We approximate $\Sigma_{\text{gas}} = 0.5 f_g \Sigma$, where f_g is the gas fraction. Since $\text{SFR} \simeq \Sigma_{\text{SFR}} \pi r_D^2$, we have $v_\infty \propto \Sigma^{1/2} r_D^{1/2} \propto \Sigma_{\text{gas}}^{1/2} r_D^{1/2} \propto \Sigma_{\text{SFR}}^{0.36} r_D^{1/2} \propto (\text{SFR}/r_D^2)^{0.36} r_D^{1/2} \propto \text{SFR}^{0.36} r_D^{-0.21}$ or

$$\begin{aligned} v_\infty &\sim 150 \text{ km s}^{-1} f_{g,0.5}^{-0.5} \left(\frac{\Sigma_{\text{SFR}}}{M_\odot \text{ yr}^{-1} \text{ kpc}^{-2}} \right)^{0.36} r_{D,1\text{kpc}}^{0.5} \\ &\sim 400 \text{ km s}^{-1} f_{g,0.5}^{-0.5} \left(\frac{\text{SFR}}{50 M_\odot \text{ yr}^{-1}} \right)^{0.36} r_{D,1\text{kpc}}^{-0.21}, \end{aligned} \quad (8)$$

which is consistent with the observation $v_\infty \propto \text{SFR}^{0.35 \pm 0.06}$ in low-redshift ULIRGs (Martin 2005) and $v_\infty \propto \text{SFR}^{0.3}$ for high-stellar-mass and high-SFR galaxies at redshift $z \sim 1$ (Weiner et al. 2009; but, see Fig. 17 from Chen et al. 2010). The observed scatter at a given SFR may be caused by different r_D , f_g , r_{rad}/r_D , v_0 , bulge and dark matter halo mass, and the time dependence of the wind properties as the stellar population evolves (see Section 3). Since we only use a simplified uniform disc model to derive equations (7) and (8), a more definitive comparison with the data should await a model with more realistic distributions of surface density, opacity, and brightness. Moreover, we can give the criterion for driving a galactic wind in terms of SFR or Σ_{SFR} . For an Eddington-limited disc, we have $F_{\text{Edd}} \propto \Sigma_{\text{gas}} \propto \Sigma_{\text{SFR}}^{0.71} \propto (\text{SFR}/r_D^2)^{0.71} \propto \text{SFR}^{0.71} r_D^{-1.43}$ or

$$\begin{aligned} F_{\text{Edd}} &\simeq 5 \times 10^{11} f_{g,0.5}^{-1} \kappa_1^{-1} \left(\frac{\Sigma_{\text{SFR}}}{M_\odot \text{ yr}^{-1} \text{ kpc}^{-2}} \right)^{0.71} L_\odot \text{ kpc}^{-2} \\ &\simeq 3 \times 10^{12} f_{g,0.5}^{-1} \kappa_1^{-1} r_{D,1\text{kpc}}^{-1.43} \left(\frac{\text{SFR}}{50 M_\odot \text{ yr}^{-1}} \right)^{0.71} L_\odot \text{ kpc}^{-2} \end{aligned} \quad (9)$$

where we have again employed the Schmidt law and $\kappa = 10 \kappa_1 \text{ cm}^2 \text{ g}^{-1}$ is the flux-mean dust opacity. Keep in mind that the dust opacity in the FIR limit is about $\kappa_{\text{FIR}} \sim 1 - 10 \text{ cm}^2 \text{ g}^{-1}$.

If we assume the galactic disc is in radial centrifugal balance with a Keplerian velocity $v_{\text{rot}} \sim \sqrt{G\pi\Sigma r}$, and we take the typical terminal velocity from equation (7) to compare to the rotation velocity at the radius r_D that $v_{\text{rot}} = v_{\text{rot}}(r = r_D)$, we have

$$v_\infty \simeq 2\sqrt{\pi/2 - 1} v_{\text{rot}} \simeq 1.5 v_{\text{rot}}. \quad (10)$$

For an exponential disc with brightness $I \propto \exp(-r/R_{\text{rad}})$, the peak rotation velocity is $v_{\text{rot}} \simeq 0.8\sqrt{G\pi\Sigma_0 R_{\text{rad}}}$, which is approximately reached at $r \simeq 1.8 R_{\text{rad}}$. This estimate is again made in the absence of galactic bulge or extended passive disc and dark matter halo. That the terminal velocity of the wind increases linearly with the galactic rotation velocity is also consistent with the observational results in Martin (2005, Fig 7). Because the flat part of the rotation curve v_c is typically comparable to the rotation velocity at the edge of the galactic disk (Sharma et al. 2011), thus we also have $v_\infty \sim 1.5 v_c$. However, the factor “1.5” in equation (10) cannot be strictly obtained due to the gravitational potential of the dark matter halo or a spherical old stellar bulge or extended passive disc, which decrease the factor of 1.5 and can cause the flow to become bound (see Section 3).

In their cosmological simulations of structure formation and IGM enrichment by galactic winds, Oppenheimer & Davé (2006) assumed a wind launch velocity $v_{\text{launch}} = 3\sigma\sqrt{\Gamma_0 - 1} \sim 3\sigma$, where σ is the galactic velocity dispersion and the factor of 3 is an assumption (see also Oppenheimer & Davé 2008; Oppenheimer et al. 2010). Taking the relation between velocity dispersion and rotation velocity $\sigma = v_{\text{rot}}/\sqrt{2}$ for the isothermal sphere (Binney & Tremaine 2008), the wind launch velocity can be written as $v_{\text{launch}} \sim 2 v_{\text{rot}}$, similar to equation (10). However, besides the initial wind launch velocity, an additional kick is given to the wind particles to overcome the halo potential, implying that the scaling of wind velocity v_∞ in Oppenheimer & Davé’s model has a higher amplitude than what we obtain from just the effect of radiation pressure on dust discussed in this paper. Nevertheless, equations (7) - (10) are essential for developing an understanding of the maximum envelope of values for v_∞ , and its dependence on the observed properties of rapidly star-forming galaxies. More physics of v_∞ and its z -dependence in the gravitational potential well of a spherical old stellar bulge or dark matter halo is presented in Section 3.

Finally, we note that the characteristic timescale for the wind to reach its asymptotic velocity is

$$t_c \sim \sqrt{r_D/(4G\Sigma)} \sim 3.5 \times 10^6 \Sigma_0^{-1/2} r_{D,1\text{kpc}}^{1/2} \text{ yr}, \quad (11)$$

which can be compared with the timescale of a bright star-forming disc: $t_* \sim M_{\text{gas}}/\text{SFR}$. Again employing the Schmidt Law, we find that

$$t_* \sim 2 \times 10^8 f_{g,0.5}^{-0.4} \Sigma_0^{-0.4} \text{ yr} \quad (12)$$

or $t_c/t_* \sim 0.02 r_{D,1\text{kpc}}^{1/2} f_{g,0.5}^{0.4} \Sigma_0^{-0.1}$. Since $t_c < t_*$, the wind can be accelerated to $\sim v_\infty$ with a timescale of t_c before the gas supply is depleted by star formation in a timescale of t_* . Note that gas recycling in the ISM will give an even longer t_* than the simple estimate $M_{\text{gas}}/\text{SFR}$.

3 EXTENDED DISC, BULGE AND DARK MATTER HALO

The galactic bulge, extended passive stellar or gaseous disc and dark matter halo are important to the wind dynamics. If we do not consider the luminosity from the galactic bulge and extended disc,² the bulge, extended disc and halo only act to decrease the asymptotic wind velocity, and may cause the wind to fall back to the disc as a “fountain flow”. For the galactic bulge we employ a truncated constant density sphere of mass M_{bulge} and spherical radius r_{bulge} . The effect of an old passive extended stellar or disc of gas can be neglected within a height scale $z \lesssim (\Sigma/\Sigma_{\text{ext}})^{1/2} R_D$ with Σ and Σ_{ext} being the surface density of nuclear disc ($r < \sqrt{2} R_{\text{rad}}$) and extended star/gas disc ($r > \sqrt{2} R_{\text{rad}}$). On the other hand, its effect at large scales is similar to the effect of an old stellar bulge, but with the following replacements: $M_{\text{bulge}} \rightarrow M_{\text{ext}}$ and $r_{\text{bulge}} \rightarrow R$, where $R = \sqrt{r^2 + z^2}$ is the cylindrical distance to the halo center, and M_{ext} is the total mass of extended disc. Note that for normal spirals and field galaxies in the local universe, their extended

² The case of a bright spherical bulge was considered in MQT05.

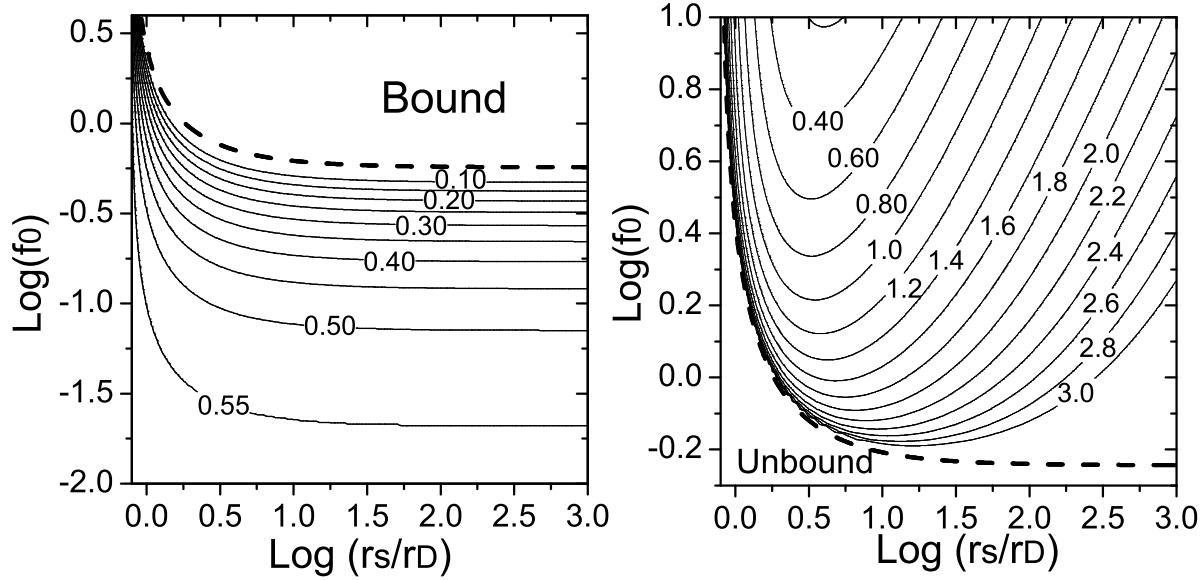


Figure 2. Contours of the asymptotic kinetic energy $(v_\infty/v_c)^2$ as a function of $f_0 = f_b + f_h$ (assuming $f_b = 0$) and $c' = r_s/r_D$ for unbound particles (*left*), and the turning point $\log_{10}(z_{\text{turn}}/r_D)$ along the pole in the case of bound particles, assuming $v_0 = 0$ (*right*). The dashed line in both panels divides “bound” and “unbound” trajectories.

star/gas discs can be very large compared to the region of more rapid star formation. As discussed in Section 2, where we identified the requirement $R_D < \sqrt{2}R_{\text{rad}}$ for wind formation, they are thus not promising to drive galactic winds via the mechanism discussed here. Instead, bulgeless galaxies without extended discs, and with very massive central concentrations of star formation — e.g., those ULIRGs with very large nuclear surface density and star formation rate, but with small Σ_{ext} — are most promising. For simplicity we do not consider the importance of an passive disc further here. Also, we adopt the NFW potential (Navarro, Frenk & White 1996) to describe the dark matter halo distribution $\rho_{\text{DM}}(r) \propto R^{-1}(R + r_s)^{-3}$, where r_s is the scale radius. For simplicity, in this section we take the uniform disc model with $r_{\text{rad}} = r_D$. The Eddington limit $\Gamma_0 = 1$ including the dark matter halo becomes

$$\frac{\pi \kappa I}{c} = 2\pi G \Sigma + \frac{1}{2} \frac{GM_{\text{halo}}}{r_s^2 f(c_{\text{vir}})} = 2\pi G \Sigma \left(1 + \frac{f_h}{2c'}\right), \quad (13)$$

where $c_{\text{vir}} = r_{\text{vir}}/r_s$, r_{vir} is the virial radius, $f(c_{\text{vir}}) = \ln(1 + c_{\text{vir}}) - c_{\text{vir}}/(1 + c_{\text{vir}})$, and

$$f_h = \frac{M_{\text{halo}}}{2\pi r_s r_D \Sigma f(c_{\text{vir}})} \sim \frac{M_{\text{halo}}}{2M_{\text{disc}}} \left(\frac{r_D}{r_s}\right) \frac{1}{f(c_{\text{vir}})}. \quad (14)$$

We introduce the parameters $c' = r_s/r_D$ and

$$f_b = \frac{1}{2} \left(\frac{M_{\text{bulge}}}{M_{\text{disc}}}\right) \left(\frac{r_D}{r_{\text{bulge}}}\right). \quad (15)$$

The parameters f_h and f_b measure the importance of the halo and bulge, respectively, in determining the dynamics of

the flow. The asymptotic velocity in terms of these parameters is (see equation [5])

$$\frac{v_\infty^2 - v_0^2}{v_c^2} = \Gamma_0 \left(1 + \frac{f_h}{2c'}\right) \frac{\pi}{2} - (1 + f_b + f_h). \quad (16)$$

Note that for $f_b, f_h \rightarrow 0$, equations (16) and (7) are equivalent.

We combine the effects of the galactic bulge and dark matter halo using the parameter $f_0 = f_h + f_b$. Assuming $\Gamma_0 = 1$, the condition for matter to be unbound is

$$f_0 < \left[\left(\frac{v_0}{v_c}\right)^2 + \left(\frac{\pi}{2} - 1\right)\right] \left(1 - \frac{\pi}{4c'}\right)^{-1}. \quad (17)$$

More generally, taking f_0 as a parameter, the terminal velocity from equation (16) is less than the value from equation (7). For the purposes of an estimate, taking $c' \sim 10$, the relation between v_∞ and $\langle v_{\text{rot}} \rangle$ becomes

$$v_\infty \simeq 1.5(1 - 1.6f_0)^{1/2} v_{\text{rot}}, \quad (18)$$

which shows that the dark matter halo potential well is too deep for particles to escape for $f_0 \gtrsim 0.6$.

Quantitatively the halo, extended disc, and bulge should have very similar effects in decreasing the outflow velocity. For simplicity, we can first neglect the bulge/disc and focus on $f_0 = f_h$ ($f_b = 0$). In this case the typical value of f_0 is given by

$$f_0 \sim 0.25 \left(\frac{M_{\text{halo}}/M_{\text{disc}}}{30}\right) \left(\frac{r_D/r_s}{1/30}\right) \left(\frac{2}{f(c_{\text{vir}})}\right), \quad (19)$$

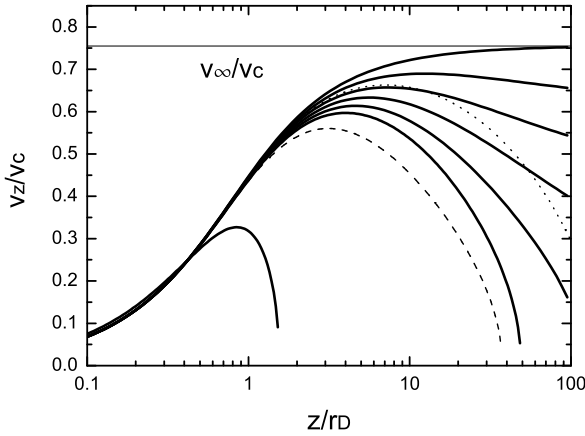


Figure 3. Outflow velocity v_z/v_c along the pole with $c' = 10$ and f_0 from top down $f_0 = 0, 0.2, 0.4, 0.6, 0.8, 1, 5$ (thick lines), $c' = 4$ (dashed line) and $c' = 100$ (dotted line) with $f_0 = 1$. The horizon line labeled as v_∞/v_c is the analytical solution as in equation (7).

where we have taken representative values of $M_{\text{halo}}/M_{\text{disc}} \sim 10-100$ (e.g., Leauthaud et al. 2011), $c' = r_s/r_D \sim 10-100$, and $f(c_{\text{vir}}) \sim 2$ (for $c_{\text{vir}} \sim 15$; Maccio et al. 2008). Thus, instead of the naive estimate without the dark matter halo in equation (10), which yields $v_\infty \simeq 1.5 v_{\text{rot}}$, we obtain $v_\infty \simeq v_{\text{rot}}$. Even so, equation (18) makes it clear that the relation $v_\infty \simeq 1.5 v_{\text{rot}}$ from equation (10) cannot be strictly achieved for Eddington-limited rapidly star-forming galaxies by the mechanism discussed in this paper since all systems have dark matter haloes, not to mention the fact that Oppenheimer & Davé’s model includes an additional kick to increase the wind terminal velocity. To the extent that the “2” in the expression of Oppenheimer & Davé’s model $v_\infty \sim 2 v_{\text{rot}}$ or “ $\sim 3-5$ ” with an extra kick is required to match observations and simulations, additional physics such as an effectively super-Eddington galaxy luminosity or supernova-driven hot flows would be necessary to add to the models here (e.g., Murray et al. 2011; Hopkins et al. 2011a,b).

The quantitative scaling relations for bound and unbound outflows, encapsulated in the factors f_0 and c' , are illustrated in Figure 2. The left panel shows contours of the asymptotic kinetic energy $(v_\infty/v_c)^2$ as a function of f_0 and $c' = r_s/r_D$ assuming $v_0 = 0$ for unbound outflows.³ The right panel of Figure 2 shows contours of $\log_{10}[z_{\text{turn}}/r_D]$, the turning point of the wind scaled to the disc radius for bound “outflows.” According to equation (19), if all else being equal, a disc with higher ratio of $M_{\text{halo}}/M_{\text{disc}}$ has larger f_0 , smaller z_{turn} , and the flow has a shorter timescale for reaching the turning point $t_{\text{turn}} \sim z_{\text{turn}}/v_c \sim t_c(z_{\text{turn}}/r_D)$ (see equation [11]). The right panel of Figure 2 shows that z_{turn}/r_D can be larger than ~ 1000 , implying that the flow reaches many tens of kpc in height above the disc before falling back towards the host on a timescale of $\sim \text{Gyr}$.

³ Increasing v_0 to $0.2v_c$ does not change the position of the contours appreciably.

Importantly, even if f_0 is large enough that the flow is bound, one may still observe an outgoing wind from a rapidly star-forming galaxy for two reasons. First, there is a region of parameter space where the time to reach the turning point t_{turn} is larger than the time for the rapidly star-forming galaxy to deplete its gas supply $t_\star = M_g/\text{SFR}$ (see equation [12]). Since $t_{\text{turn}}/t_\star \sim (z_{\text{turn}}/r_D)t_c/t_\star$ (see equation [11]), $z_{\text{turn}}/r_D \gtrsim 60r_{D,1\text{kpc}}^{-1/2}f_{g,0.5}^{-0.4}\Sigma_0^{0.1}$ is required for $t_{\text{turn}}/t_\star \gtrsim 1$. Second, an observable flow along the line of sight to a non-edge-on disc can have a maximum velocity v_{max} that is comparable to v_∞ in equation (7), even though the flow is bound on large scales (z_{turn}) by the dark matter halo. Figure 3 shows the one-dimensional outflow velocity v_z/v_c along the pole with various f_0 and c' . In the bound case, the maximum outflow velocities v_{max} peak around $1-10r_D$ before decreasing to much lower values. The maximum v_{max} is still comparable to v_∞ in the absence of a halo or bulge or extended disc, except for very large $f_0 \gtrsim 5$ (see equation [19]). The velocity of the flow before changing sign and falling back to the host galaxy is time-dependent and approximately reaches its maximum at a time $\sim t_c$ (equation [11]).

The fact that $t_{\text{turn}} > t_\star$ and that v_{max} approaches a few $\times v_{\text{rot}}$ together imply that if galaxies are selected as bright rapidly star-forming galaxies, they may appear to have unbound outflows even though the gas is in fact bound on large scales by the dark matter halo potential. Indeed, Figure 3 implies that rapidly star-forming galaxies with bound flows may exhibit a rough correlation of the form $v_{\text{max}} \sim 1-1.5 v_{\text{rot}}$.

4 3-DIMENSIONAL WINDS AND MASS LOSS RATE

So far we have focused on the forces along the polar z -axis. Figure 4 shows 2-dimensional (2D) projections of the 3D orbits of test particles accelerated by radiation pressure and gravity, as well as their constant time surfaces above a uniform disc, starting from an initial height $z_0 = 0.1r_D$ and initial radii $r_0 = 0, 0.1r_D, 0.2r_D, 0.3r_D, \dots$, both with and without an NFW potential, and with no galactic bulge or extended passive disc. The opening angles of particle trajectories are formed because particles initially co-rotate in the disc with an angular momentum v_{rot}^2/r except for particles along the z -axis. In the absence of a halo, the upper middle panel shows that winds can be driven from part of the disc region (e.g., $r_0 > 0.5r_D$ in this panel) even when the disc is sub-Eddington ($\Gamma_0 = 0.88$), while the upper right panel shows the wind can also be launched even beyond the edge of bright disk ($r > r_D$) in a super-Eddington case ($\Gamma_0 = 5$). The lower panels show that the character of the flow changes significantly as f_0 increases from 0.2, to 0.6, to 1.0 (left to right; compare with equation [19]). For the case $f_0 = 0.2$, the wind is clearly unbound. For $f_0 = 0.6$, particles emerging near the z -axis are accelerated to very large vertical distances, whereas particles emerging from the outer disc region fall back to the disc rapidly. A more massive halo with $f_0 = 1.0$ produces only a “fountain flow” in which particles fall back to the disc with a timescale of $\sim 0.1-1 \text{ Gyr}$. Moreover, Figure 5 gives the 3D orbit vertical component v_z evolution of the particles driven from different disc regions.

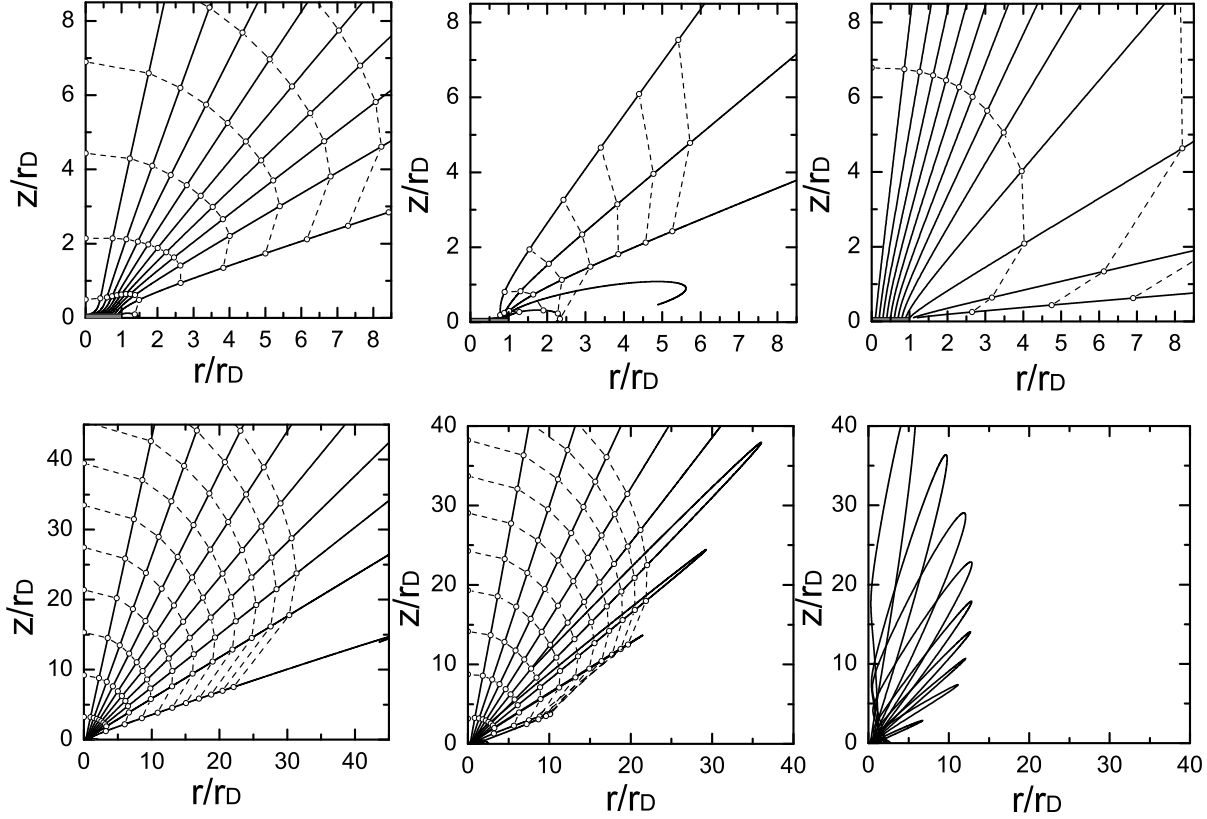


Figure 4. The particle orbits from the disc without (upper panels) and with (lower panels) NFW potential. Solid lines show 2-dimensional projections of the 3-dimensional orbits. Upper panels, left to right, we take $\Gamma_0 = 1, 0.88$ and 5 . Particles are initially located at disc surface $z_0 = 0.1r_D$ with $r_0/r_D = 0, 0.1, 0.2, 0.3, 0.4, \dots 1.0$. In the upper middle panel trajectories with initial radii $r_0/r_D < 0.5$ are skipped because they are bound, while in the upper right panel extra trajectories with initial radii $r_0/r_D = 1.1$ and 1.2 are also plotted. The particle positions and constant time surfaces are labeled at $t/t_c = 2, 4, 6, 8, 10, \dots$, where $t_c = \sqrt{r_D/(4G\Sigma)}$ (eq. 11). Lower panels, left to right: $f_0 = 0.2, 0.6, 1.0$ with $\Gamma_0 = 1$ and $c' = 10$. Constant time surfaces are marked at $t/t_c = 5, 10, 15, 20, 25, \dots$.

For a face-on disc, the velocity v_z of the wind is just the velocity along the line of sight. The maximum velocities are reached roughly at $t \sim t_c$. Also, the maximum and terminal velocities of particles from the outer disc region are smaller than those from the inner disc region. As in Figure 4, matter from the outer region of the disc can be bound by the halo's gravitational potential even though matter from the inner region is unbound.

To estimate the rate of mass ejection and mass loss rate from Eddington-limited discs, we first calculate that the Eddington flux and luminosity are

$$F_{\text{Edd}} = 2\pi c G \Sigma / \kappa \sim 3 \times 10^{12} \Sigma_0 \kappa_1^{-1} L_\odot \text{ kpc}^{-2}, \quad (20)$$

and

$$L_{\text{Edd}} = \pi r_{\text{rad}}^2 F_{\text{Edd}} \sim 10^{13} \left(\frac{r_{\text{rad}}}{r_D} \right)^2 \Sigma_0 \kappa_1^{-1} r_{D,1\text{kpc}}^2 L_\odot, \quad (21)$$

respectively.

The total mass ejection rate from the disc surface \dot{M}_{ej} is a local quantity measured on a disc scale height

h_{disc} . The disc, bulge, and dark matter halo gravitational forces at the disc scale height h_{disc} estimated at $(R, z) \sim (0, h_{\text{disc}})$ as $f_{\text{disc}} \sim 2\pi G \Sigma_{\text{(disc)}}$, $f_{\text{bulge}} \sim \pi G \rho_{\text{bulge}} h_{\text{disc}}$, and $f_{\text{halo}} \sim G M_{\text{halo}} / [2r_s^2 f(c_{\text{vir}})]$ respectively. Taking the case of $\rho_{\text{bulge}} h_{\text{disc}} \ll \Sigma_{\text{disc}}$, the gravity of the bulge can be neglected at h_{disc} since $f_{\text{bulge}} \ll f_{\text{disc}}$. Similarly, since the ratio of the halo to the disc gravity $f_{\text{halo}}/f_{\text{disc}} \sim 4 \times 10^{-3} \left(\frac{r_D/r_s}{1/30} \right)^2 \left(\frac{M_{\text{halo}}/M_{\text{disc}}}{30} \right) \left(\frac{2}{f(c_{\text{vir}})} \right) \ll 1$, the halo can also be neglected on the disc height scale h_{disc} . Therefore \dot{M}_{ej} can be determined only by the disc, and be estimated in the absence of bulge and halo from the integrated momentum equation. In the single-scattering limit (i.e., all photons are scattered/absorbed once in the wind; e.g., MQT05), an estimate of \dot{M}_{ej} is

$$\dot{M}_{\text{ej}} v_{\infty, f_0=0} \sim L_{\text{Edd}} / c, \quad (22)$$

where $v_{\infty, f_0=0}$ is the terminal velocity of the flow without a bulge, extended passive disc or dark matter halo (equation [7]). Since $v_{\infty, f_0=0}$ is an upper limit to the velocity of the

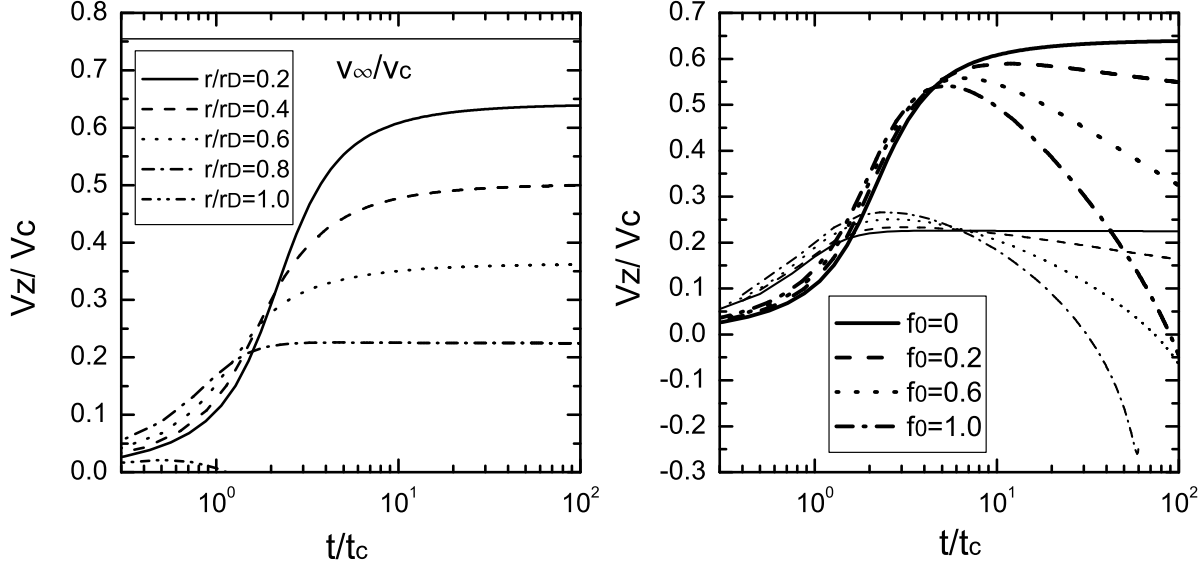


Figure 5. *Left panel:* The time evolution of v_z/v_c for $r/r_D = 0.2$ to 1.0 starting with $z/r_D = 0.1$ and $\Gamma_0 = 1$. The horizon line v_∞/v_c is the same as Figure 3. *Right panel:* the velocity v_z/v_c starting from $(r/r_D, z/z_D) = (0.2, 0.1)$ (thick lines) and $(0.8, 0.1)$ (thin lines) with different values f_0 for the dark matter potential with $c' = 10$ and $\Gamma_0 = 1$.

flow (valid as $f_0 \rightarrow 0$; see equation [18]), equation (22) is only approximate. Nevertheless, to the extent that v_{\max} is of order $v_{\infty, f_0=0}$ (see Figure 3), equation (22) should yield an order-of-magnitude estimate of the mass loss rate from the disc itself. Combining equations (7) and (22) we have

$$\dot{M}_{\text{ej}} \sim 3 \times 10^2 \left(\frac{r_{\text{rad}}}{r_D} \right)^2 \Sigma_0^{1/2} \kappa_1^{-1} r_{D, 1\text{kpc}}^{3/2} M_\odot \text{ yr}^{-1}, \quad (23)$$

which is similar to observational results (e.g., Martin 2005, 2006). Using equations (8) and (9), the mass ejection rate is also given by

$$\dot{M}_{\text{ej}} \sim 6 \times 10^2 f_{g, 0.5}^{-0.5} \kappa_1^{-1} r_{D, 1\text{kpc}}^{0.79} \left(\frac{\text{SFR}}{50 M_\odot \text{ yr}^{-1}} \right)^{0.36} M_\odot \text{ yr}^{-1}. \quad (24)$$

Using $L = \epsilon c^2 \text{SFR}$ to calculate the luminosity of a rapidly star-forming galaxy (e.g., Kennicutt 1998), where $\epsilon_{-3} = \epsilon/10^{-3}$ is the efficiency with which star formation converts mass into radiation, the single-scattering estimate for the ratio of the mass ejection rate to the SFR is

$$\frac{\dot{M}_{\text{ej}}}{\text{SFR}} \sim \frac{\epsilon c}{v_{\infty, f_0=0}} \sim 0.8 \epsilon_{-3} \Sigma_0^{-1/2} r_{D, 1\text{kpc}}^{-1/2}, \quad (25)$$

which implies that radiation pressure drives more matter from discs in low-mass galaxies (see MQT05): for example, $\dot{M}_{\text{ej}}/\text{SFR} \gtrsim 10$ for $\Sigma r_D \lesssim 3.1 \times 10^4 M_\odot \text{ pc}^{-1}$. However, as low mass galaxies are usually the most dark matter halo dominated with higher ratio of $M_{\text{halo}}/M_{\text{disc}}$ (Persic et al. 1996), or larger f_0 (see equations [17] and [19]), the matter lost from low mass discs may not escape the halo potential, and will fall back on the timescale t_{turn} (see the right panel of Figure 2). Otherwise, some additional physical mechanism beyond that described in this paper (e.g.,

a supernova-heated wind) is needed to unbind it from the halo.

The quantity \dot{M}_{ej} in the above expressions is the rate at which matter is ejected from the disc in either a bound or unbound flow. In the former case, as discussed in Section 3, the outflow reaches a maximum outward velocity v_{\max} before returning to the disc on a timescale t_{turn} , which in many cases is $> t_*$. In the case of an unbound outflow, \dot{M}_{ej} is an estimate for the mass loss rate from the halo as a whole on large scales. As emphasized in Section 3, the critical parameter determining whether or not the flow is bound or unbound is f_0 (equations [17] and [19]).

For a totally unbound outflow that escapes the gravitational potential, the asymptotic mass loss rate of the outflow from the large-scale bulge and halo gravitational potential (\dot{M}_∞) should be the same as the mass loss rate from the disc \dot{M}_{ej} : $\dot{M}_\infty = \dot{M}_{\text{ej}}$. However, in the bound and partially bound cases (e.g., see Figure 4 as examples), \dot{M}_∞ should only be a fraction of \dot{M}_{ej} such that $\dot{M}_{\text{ej}} > \dot{M}_\infty \geq 0$, and the ratio $\xi = \dot{M}_\infty/\dot{M}_{\text{ej}}$ depends on the disc Eddington ratio Γ and the depth of the large scale gravitational potential. Figure 6 shows $\xi(\Gamma)$ for NFW haloes with $c' = 10$ and $f_0 = 0, 0.2, 0.6$ and 1 . We calculate $\xi(\Gamma)$ by following the trajectories of test particles, as in Figure 4, launched from various radii just above the disc surface. Because the disc is assumed to have uniform surface density, $\xi(\Gamma)$ is the ratio of the disc area over which particles terminally escape the large scale halo to the total disc area. We find that $\xi(\Gamma)$ is a strongly increasing function of Γ , and that it decreases substantially as f_0 is increased. For $f_0 = 0.2$ and 0.6 (see equation [19]), $\xi(\Gamma) \simeq 0.8$ and 0.65 at $\Gamma = 1$, respectively, showing that for typical dark matter halo properties $\sim 60\% - 80\%$ of the

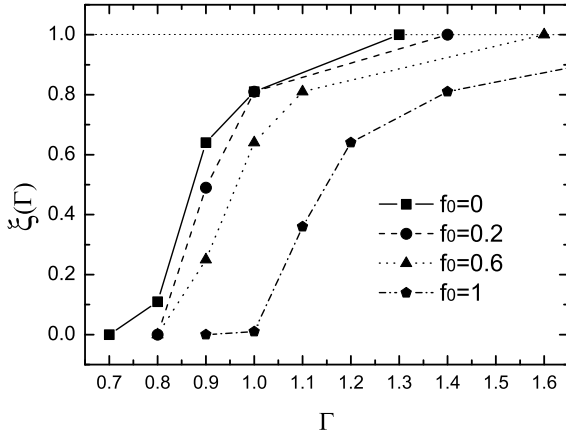


Figure 6. Ratio of the asymptotic mass loss rate from the gravitational potential (\dot{M}_∞) and the initial mass loss rate from the disc (\dot{M}_{ej}), $\xi(\Gamma) = \dot{M}_\infty/\dot{M}_{\text{ej}}$, as the function of disc Eddington ratio Γ , assuming a NFW dark matter potential as in Figure 4 with $f_0 = 0, 0.2, 0.6$ and 1 with $c' = 10$.

matter ejected from the disc is completely unbound for Eddington discs, whereas the remainder forms a fountain flow. The totally unbound wind (i.e., $\xi = 1$) can be only approached for super-Eddington discs. A more complete study of the asymptotic mass loss should follow the hydrodynamics of the outflow instead of taking the test particle approximation.

5 CONCLUSIONS & DISCUSSION

In this paper we study the large-scale winds from uniformly bright self-gravitating discs radiating near the Eddington limit. Different from the spherical case, where the Eddington ratio $\Gamma = f_{\text{rad}}/f_{\text{grav}}$ is a constant with distance from the source, for discs Γ increases to a maximum of twice its value at the disc surface (Section 2). As a result, such discs radiating at (or even somewhat below; see Figures 1 and 4) the Eddington limit are unstable to driving large-scale winds by radiation pressure.

We quantify the characteristics of the resulting outflow in the context of Eddington-limited star-forming galaxies, motivated by the work of TQM05 who argued that radiation pressure on dust is the dominant feedback process in rapidly star-forming galaxies. We find that the asymptotic terminal velocity along the polar direction from discs without a stellar bulge, extended passive disc or dark matter halo is $v_\infty \sim \sqrt{4\pi G \Sigma r_D} \sim 1.5 v_{\text{rot}}$, where r_D is the disc radius, Σ is the surface density, v_{rot} is the disc rotation velocity (see equations [7] and [10]), and may range from $\sim 50 - 1000 \text{ km s}^{-1}$ for rapidly star-forming galaxies, depending on the system considered. Furthermore, by employing the observed Schmidt law, we find that $v_\infty \propto \text{SFR}^{0.36} r_D^{-0.21}$ (see equation [8]). These results, in the absence of dark matter halo and bulge, or extended passive disc, are in agreement with recent observations (e.g., Martin 2005, 2006; Weiner et al. 2009; see also Chen et al. 2010). The typical mass loss rate

from an Eddington-limited disc in the single-scattering limit is given by equation (23) and suggests these outflows may efficiently remove mass from the disc (equation [25]).

However, both wind velocities and outflow rates can be significantly decreased by the presence of a spherical old stellar bulge or extended gravitational disc or dark matter halo potential (Section 3). Deeper or more extended spherical gravitational potentials cause the flow to be bound on large scales, and to produce only “fountain flows” where particles fall back to the disc on a typical timescale of $\sim 0.1 - 1 \text{ Gyr}$, depending on the parameters of the system considered (see Figures 2-6). The criterion for the flow to become bound along the polar direction is given in equation (17). For typical values of the parameter f_0 (see equation [19]), we find that the winds from rapidly star-forming galaxies can be either bound or unbound (see Figure 2). As an example, for $f_0 \simeq 0.25$ in equation (19), the asymptotic velocity of the wind is decreased by a factor of $\simeq 0.7$ from the case neglecting the dark matter halo completely (compare equations [10] and [18]), from $\simeq 1.5 v_{\text{rot}}$ to $\simeq v_{\text{rot}}$. However, for $f_0 > 0.6$ the asymptotic velocity goes to zero along the z -axis and the flow becomes bound on large scales. A more elaborate 3D calculation shows that a totally unbound wind from a 2D disc surface can only be approached at super-Eddington discs, otherwise the outflow asymptotic mass loss rate from the large scale gravitational potential \dot{M}_∞ is only a fraction of mass ejection rate from the disc \dot{M}_{ej} (Figure 6).

Importantly, even in the limit of bound fountain flows, if the timescale t_{turn} for reaching the turning point z_{turn} is longer than the lifetime of the rapidly star-forming galaxy t_\star (equation [12]), one may still observe an outward going wind while the rapidly star-forming galaxy is active and bright. The maximum positive velocity of the flow v_{max} along the line of sight for non-edge-on discs is still correlated with v_{rot} of the disc (see Section 3). These facts may complicate the inference from observations of winds that they are unbound from the surrounding large-scale dark matter halo.

More detailed work is required to fully assess radiation pressure on dust as the mechanism for launching cool gas from rapidly star-forming discs. Extra observational evidence beyond the relation $v_\infty \propto \text{SFR}^{0.36}$ should certainly be added to verify the radiation-driven model from more realistic discs instead of the idealized model of uniform discs we consider in this paper. Equations (7) and (8) also give testable relations between v_∞ and galactic surface density Σ , which can also be used to compare with observations of cold winds from galaxies with observed radii and masses. One key ingredient of our model is that galaxies should approach the dust Eddington limit. TQM05 proposed that a significant fraction of the radiation from ULIRGs should be produced by an Eddington-limited rapidly star-forming galaxy (see also the discussion of the dust Eddington limit in Hopkins et al. 2010). If so, the dust-driven mechanism discussed in this paper can be applied to the winds from ULIRG discs. Moreover, galaxies at high redshifts are more active and thus potentially more likely to approach the Eddington limit (e.g., MQT05). Take the data on extreme starburst Arp220 in Downes & Solomon (1998) as a case study. The surface density of Arp 220 West (East) core region is $\Sigma \approx 20 \text{ g cm}^{-2}$ (18 g cm^{-2}), corresponding to a FIR-thick disc with an Eddington ratio of $\Gamma \approx 0.3(\kappa/10 \text{ cm}^2 \text{ g}^{-1})$ ($\Gamma \approx 0.1(\kappa/10 \text{ cm}^2 \text{ g}^{-1})$). Ignoring the observa-

tional uncertainties in Γ , the sub-Eddington luminosities imply that the outflow from the Arp 220 cores may be caused by other mechanisms such as the energy and momentum input from supernovae rather than just radiation pressure on dust (Chevalier & Clegg 1985; Strickland & Heckman 2009; Hopkins et al. 2011a,b).

The main limitations of our model of radiation-driven wind presented here are that (1) we consider only discs with constant brightness and surface density, (2) we do not compute the hydrodynamics of the flow, but instead treat the outflow in the test-particle limit, and (3) we ignore other physical mechanisms, which may act in concert with radiation pressure (MQT05; Murray et al. 2011). The general case, with hydrodynamics, realistic disc brightness, surface density, and dust opacity profiles will modify the picture presented here. Such an effort is underway. However, the basic conclusion that uniformly bright self-gravitating discs radiating near the Eddington limit are able to drive large-scale winds — particularly in the high- Σ limit in rapidly star-forming galaxies (see Section 2) — should not be fundamentally changed by more elaborate considerations. Indeed, although we have specialized the discussion to rapidly star-forming galaxies and dust opacity, the instability derived in Section 2 is of general applicability.

ACKNOWLEDGMENTS

We thank the anonymous referee for his/her very useful comments that have allowed us to improve our paper. We also thank Norman Murray, Crystal Martin, Romeel Davé, Paul Martin, and especially Mark Krumholz and Eliot Quataert for many stimulating discussions and for a critical reading of the text. This work is supported by NASA grant # NNX10AD01G.

REFERENCES

- Andrews B. H., Thompson T. A., 2011, *ApJ*, 727, 97
Aguirre A., Hernquist L., Schaye J., Katz N., Weinberg D. H., Gardner J., 2001, *ApJ*, 561, 521
Binney J., Merrifield M., eds, 1998, *Galactic Astronomy*. Princeton Univ. Press, Princeton, NJ
Binney J., Tremaine S., 2008, *Galactic Dynamics*, 2nd edn. Princeton Univ. Press, Princeton, NJ
Chen Y.-M., Tremonti C. A., Heckman T. M., Kauffmann G., Weiner B. J., Brinchmann J., Wang J., 2010, *AJ*, 140, 445
Chevalier R. A., Clegg A. W., 1985, *Nature*, 317, 44
Davé R., Oppenheimer B. D., Sivanandam S., 2008, *MNRAS*, 391, 110
Dekel A., Silk J., 1986, *ApJ*, 303, 39
De Young, D. S., Heckman, T. M., 1994, *ApJ*, 431, 598
Downes D., Solomon P. M., 1998, *ApJ*, 507, 615
Erb D. K., Shapley A. E., Pettini M., Steidel C. C., Reddy N. A., Adelberger K. L., 2006, *ApJ*, 644, 813
Finlator K., Davé R., 2008, *MNRAS*, 385, 2181
Fujita A., Martin C. L., Mac Low M.-M., New K. C. B., Weaver R., 2009, *ApJ*, 698, 693
Heckman T. M., Armus L., Miley G. K., 1990, *ApJS*, 74, 833
Heckman T. M., Lehnert M. D., Armus L., in Shull, J. M., Thronson, H. A. Jr., eds, *The Environment and Evolution of Galaxies* P. 455 (Kluwer, Dordrecht)
Heckman T. M., Lehnert M. D., Strickland D. K., Armus L., 2000, *ApJ*, 129, 493
Hopkins P. F., Quataert E., Murray N., 2011, *MNRAS*, 417, 950
Hopkins P. F., Quataert E., Murray N., 2011, *arXiv*: 1110.4638
Hopkins P. F., Murray N., Quataert E., Thompson T. A., 2010, *MNRAS*, 401, 19
Kennicutt Jr. R. C. 1998, *ApJ*, 498, 541
Leauthaud A. 2011, *arXiv*: 1104.0928
Macciò A. V., Dutton A. A., van den Bosch F. C., 2008, *MNRAS*, 391, 1940
Martin C. L. 1999, *ApJ*, 513, 156
Martin C. L. 2005, *ApJ*, 621, 227
Martin C. L. 2006, *ApJ*, 647, 222
Merritt D., Graham A. W., Moore B., Diemand J., Terzić B. 2006, *AJ*, 132, 2685
Murray N., Quataert E., Thompson T. A., 2005, *ApJ*, 618, 569 (MQT05)
Murray N., Ménard B., Thompson T. A., 2011, *ApJ*, 735, 66
Navarro J. F., Frenk C. S., White S. D. M., 1996, *ApJ*, 462, 563
Oppenheimer B. D., Davé R., 2006, *MNRAS*, 373, 1265
Oppenheimer B. D., Davé R., 2008, *MNRAS*, 387, 577
Oppenheimer B. D., Davé R., Kereš, D., Fardal M., Katz N., Kollmeier J. A., Weinberg D. H., 2010, *MNRAS*, 406, 2325
Peeples M. S., Shankar F., 2011, *MNRAS*, tmp, 1387
Pettini M., Shapley A. E., Steidel C. C., Cuby, J.-G., Dickinson M., Moorwood A. F. M., Adelberger K. L., Gialalisco M., 2001, *ApJ*, 554, 981
Pettini M., Rix S. A., Steidel C. C., Hunt M. P., Shapley A. E., Adelberger K. L., 2002, *Ap&SS*, 281, 461
Persic, M., Salucci, P., Stel, F., 1996, *MNRAS*, 281, 27
Proga D. 2000, *ApJ*, 538, 684
Proga D. 2003, *ApJ*, 585, 406
Proga D., Stone J. M., Drew J. E., 1998, *MNRAS*, 295, 595
Proga D., Stone J. M., Drew J. E., 1999, *MNRAS*, 310, 476
Rupke D. S., Veilleux S., Sanders D. B., 2005, *ApJS*, 160, 115
Rybicki G. B., Lightman A. P., 1979, *Radiative Processes in Astrophysics*. Wiley, New York
Sawicki M. et al. 2008, *ApJ*, 687, 884
Shapley A. E., Steidel C. C., Pettini M., Adelberger K. L., 2003, *ApJ*, 588, 65
Sharma M., Nath B. B., Shchekinov Y., 2011, *ApJ*, 736, 27L
Springel V., Hernquist L., 2003, *MNRAS*, 339, 312
Strickland D. K., Stevens I. R., 2000, *MNRAS*, 314, 511
Strickland D. K. et al., 2002, *ApJ*, 568, 689
Strickland D. K., Heckman T. M., 2009, 697, 2030
Tajima Y., Fukue J., 1996, *PASJ*, 48, 529
Tajima Y., Fukue J., 1998, *PASJ*, 50, 483
Thompson T. A., Quataert E., Murray N., 2005, *ApJ*, 630, 167 (TQM05)
Thilker D. A. et al., 2005, *ApJ*, 619, L67
Tremonti C. A. et al., 2004, *ApJ*, 613, 898
Weiner B. J. et al., 2009, *ApJ*, 692, 187